

Intelligence Indirect Vector Control of a DFIG based Wind Turbines

Habib Benbouhenni

Laboratoire LAAS, Ecole Nationale Polytechnique d'Oran Maurice Audin, Oran, Algérie.
Email: habib0264@gmail.com

Received: September 2018

Revised: December 2018

Accepted: March 2019

ABSTRACT:

An intelligence Indirect Vector Control (IVC) of a Doubly Fed Induction Generator (DFIG) by using a five-level inverter with space vector modulation (5L-SVM) strategy is proposed in this article. The novelty of the proposed intelligence strategy is an Artificial Neural Network (ANN), which is utilised for the IVC command of the DFIG. In this research, ANN has been replaced with the hysteresis comparators of the 5L-SVM technique. The backpropagation process is used for the training process of the ANN. By using the ANN outputs, the SVM-ANN strategy develops command pulses for the five-level inverter. Subsequently, the proposed intelligence strategy is implemented in the MATLAB/Simulink platform and the effectiveness is analysed by comparing different tests. The simulation and comparison results have demonstrated the superiority of the proposed approach and confirmed the potential of the proposed system for solving the problem.

KEYWORDS: Indirect Vector Control, DFIG, ANN, 5L-SVM, SVM-ANN.

1. INTRODUCTION

Vector control (VC) is the most popular command scheme used in the doubly fed induction generator (DFIG) based wind turbine systems (WTSS) [1], [2]. This command is simple and easy to implement. On the other hand, the major disadvantages of some DFIG controlled by VC command are the power ripples and high harmonic distortion of the rotor current. In this command strategy, decoupling between the d-axis and q-axis current is achieved by using a feed-forward compensation; while making the DFIG model simple and enabling the use of the PI controllers. Nevertheless, this command structure strongly depends on machine parameters. It uses multiple loops and requires much command-effort to guarantee the structure stability over the total velocity range [3].

Conventionally, space vector modulation (SVM) is widely used for command AC machine. This strategy reduces the harmonic distortion of current, flux and torque ripples compared to pulse width modulation (PWM). On the other hand, the principle of the SVM technique is detailed in [4-6]. Since the SVM technique is based on the principles of space vectors; sector and angle calculations are required [7-8]. To solve the problems of the SVM technique, we proposed a new SVM technique based on a calculation of maximum and minimum of three-phase voltages (V_a , V_b , V_c) [9]. The advantages of the proposed SVM technique are listed as following; it does not need to calculate

the sector and angle, it is simple to implement, and it gives a strong performance for the real-time feedback command compared with PWM inverter. In [10], the author proposes a new two-level SVM inverter based on the ANN controller named (NSVM) to command active and reactive powers of a DFIG. This strategy has reduced THD value of the stator current, power ripples. It also has simple modulation scheme and is easy to implement.

In this paper, we apply the IVC command on the DFIG based wind turbine systems using five-level NSVM (5L-NSVM) strategy compared to the 5L-SVM.

2. DFIG ODEL

A model of the DFIG is presented in literature [11], [12]. In the Park reference frame, the rotor and stator voltage equations of the DFIG are given as follows:

$$\begin{cases} V_{ds} = R_s I_{ds} + \frac{d}{dt} \psi_{ds} - \omega_s \psi_{qs} \\ V_{qs} = R_s I_{qs} + \frac{d}{dt} \psi_{qs} + \omega_s \psi_{ds} \\ V_{dr} = R_r I_{dr} + \frac{d}{dt} \psi_{dr} - \omega_r \psi_{qr} \\ V_{qr} = R_r I_{qr} + \frac{d}{dt} \psi_{qr} + \omega_r \psi_{dr} \end{cases} \quad (1)$$

The rotor and stator flux can be expressed as:

$$\begin{cases} \psi_{ds} = L_s I_{ds} + M I_{dr} \\ \psi_{qs} = L_s I_{qs} + M I_{qr} \\ \psi_{dr} = L_r I_{dr} + M I_{ds} \\ \psi_{qr} = L_r I_{qr} + M I_{qs} \end{cases} \quad (2)$$

The stator reactive and active powers can be expressed as:

$$\begin{cases} P_s = \frac{3}{2}(V_{ds} I_{ds} + V_{qs} I_{qs}) \\ Q_s = \frac{3}{2}(V_{qs} I_{ds} - V_{ds} I_{qs}) \end{cases} \quad (3)$$

The electromagnetic torque is expressed as:

$$T_e = pM(I_{dr}I_{qs} - I_{qr}I_{ds}) \quad (4)$$

$$T_e = T_r + J \cdot \frac{d\Omega}{dt} + f \cdot \Omega \quad (5)$$

- T_r : is the load torque.
- T_e : is the electromagnetic torque.
- Ω : is the mechanical rotor speed.
- J : is the inertia.
- f : is the viscous friction coefficient.
- p : is the number of pole pairs.
- P_s : is the stator active power.
- Q_s : is the stator reactive power.

- V_{dr} , and V_{qr} : are rotor voltages.
- V_{qs} and V_{ds} : are stator voltages.
- I_{dr} , and I_{qr} : are rotor currents.
- I_{ds} and I_{qs} : are stator currents.
- ψ_{dr} and ψ_{qr} : are rotor fluxes.
- ψ_{ds} and ψ_{qs} : are stator fluxes.
- L_r : is the inductance own rotor
- L_s : is the inductance own rotor
- M : is the mutual inductance.
- R_r : is the resistances of the rotor windings.
- R_s : is the resistances of the stator windings.
- ω_s : is the electrical pulsation of the stator .
- ω_r : is the electrical pulsation of the rotor.

3. FIVE-LEVEL NEURAL SPACE VECTOR MODULATION

Basic principle of 5L-SVM technique is depicted in Fig. 1. However, this technique gives more power ripples, torque ripple and high distortion harmonic of stator current. In order to improve the 5L-SVM performances, a complimentary use of the artificial neural networks (ANN) is proposed. The principle of neural space vector modulation (NSVM) is like to conventional SVM strategy. The difference is using ANN controllers to replace the hysteresis comparators. As shown in Fig. 2. ANN is newly getting increasing stress in drive command applications. The main preference of the ANN controller is that it is easy to implement the command, as well as, the capability of generalization [12]. The block diagram of ANN controllers-based hysteresis comparators is shown in Fig. 3. The structures of Layer 1 and layer 2 are shown in Fig. 4 and Fig. 5 respectively.

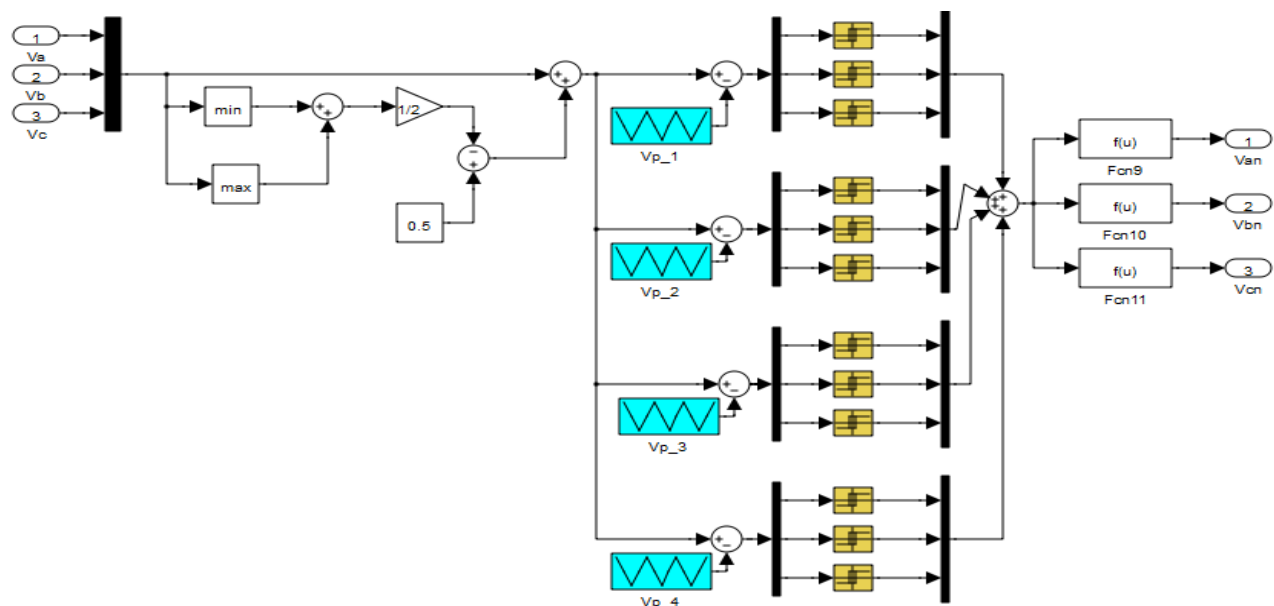


Fig. 1. Five-level SVM inverter.

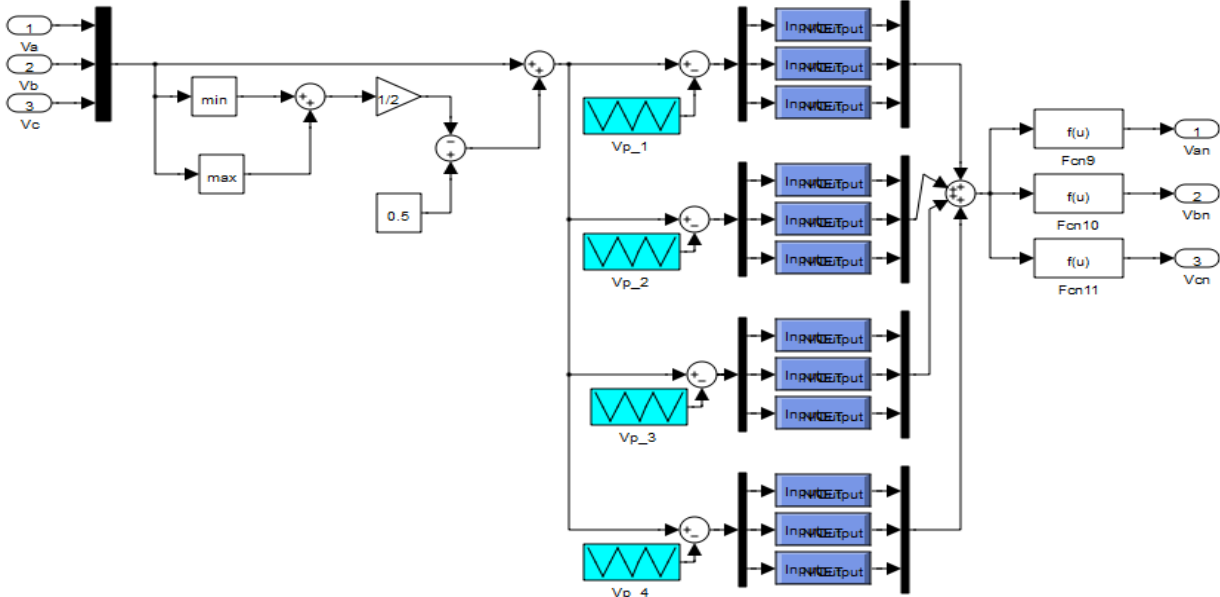


Fig. 2. Five-level NSVM inverter.

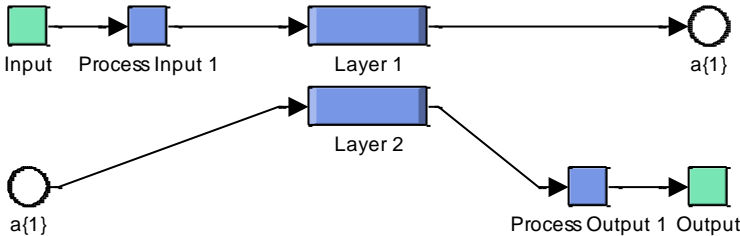


Fig. 3. Structure of ANN hysteresis comparators.

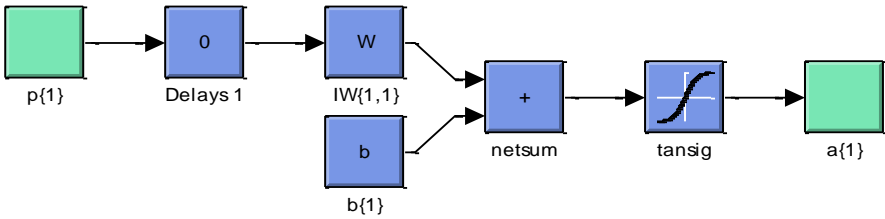


Fig. 4. Layer 1.

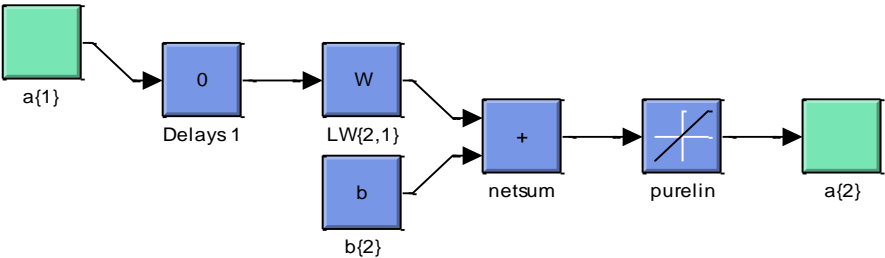


Fig. 5. Layer 2.

The convergence of the network in summer has been obtained by using the value of the parameters grouped in the Table 1.

Table 1. Parameters of the LM for hysteresis comparators.

| Parameters of the LM | Values |
|---|--------------------------|
| Number of hidden layer | 08 |
| TrainParam.show | 50 |
| TrainParam.eposh | 1000 |
| TrainParam.Lr | 0.005 |
| Coeff of acceleration of convergence (mc) | 0.9 |
| TrainParam.goal | 0 |
| TrainParam.mu | 0.9 |
| Functions of activation | Tensing, Purling, gensim |

The five-level NSVM (5L-NSVM) inverter minimizes the THD value of rotor current, as well as, the power ripples compared to conventional 5L-SVM inverter. However, this strategy has simple scheme modulation, and it is easy to implement.

4. INDIRECT VECTOR CONTROL WITH 5L-NSVM

Indirect Vector command (IVC) have been widely used for large scale command systems. The IVC command and operation of doubly fed induction generator have been the subject of intense research during last few years. However, IVC command using proportional-integral (PI) controllers is the traditional command technique used for doubly fed induction generator based wind turbine systems. In this command, the decoupling between d-axis and q-axis current is achieved with feedforward compensation, and thus the DFIG model becomes less difficult and PI controllers can be used. Nevertheless, this command scheme is simple command and easy to implement. On the other hand, the principle of the IVC command scheme is detailed in [13-16]. However, the IVC command with five-level SVM modulation, which is designed to command stator active power and reactive power of the induction generator, is shown in Fig. 6. However, the IVC with 5L-SVM strategy gives more total harmonic distortion (THD) of rotor current, torque ripple, reactive power and active power ripples. On the other hand, the structure interne of IVC command is shown in Fig. 7.

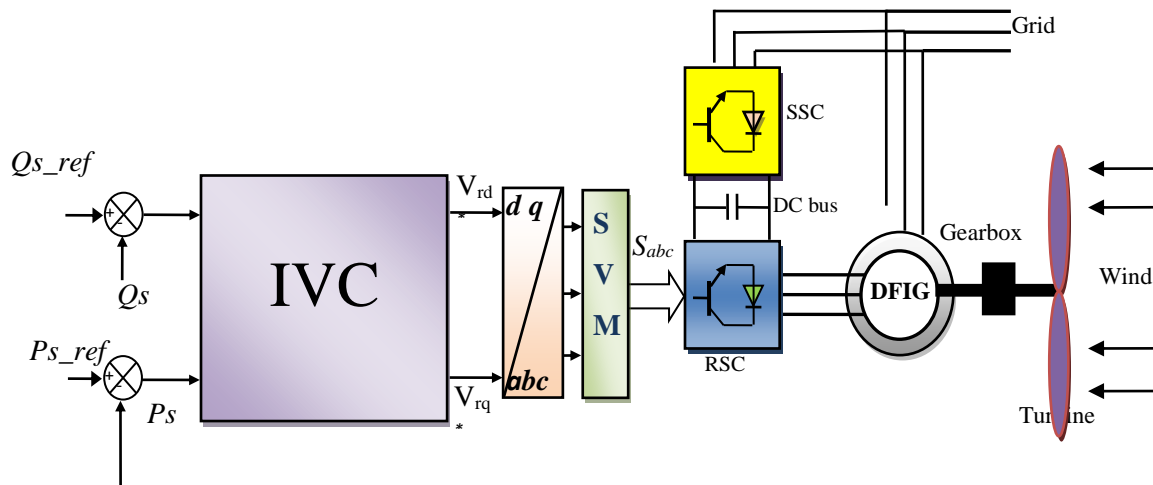


Fig. 6. Block diagram of DVC control with five-level SVM.

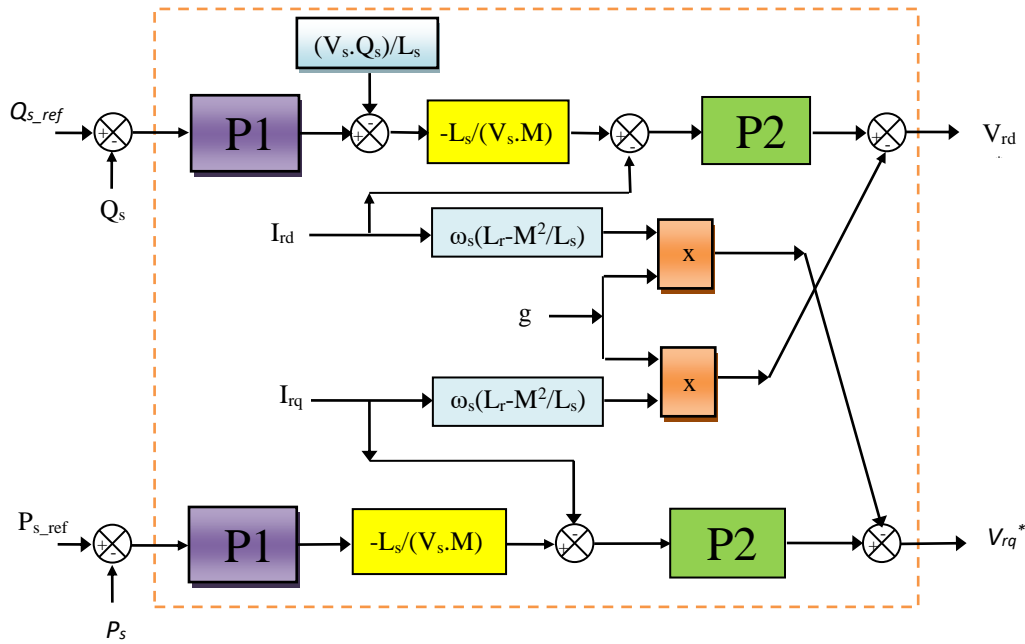


Fig. 7. Structure of IVC scheme.

To minimize the THD of rotor current, power ripples, electromagnetic torque ripple, we have applied the 5L-NSVM inverter. However, IVC command with five-level NSVM (IVC-5L-SVM) has a simple

command, and it is easy to implement. It also reduces the power ripples. The proposed IVC-5L-NSVM, which is designed to command active and reactive power of the DFIG, is shown in Fig. 8.

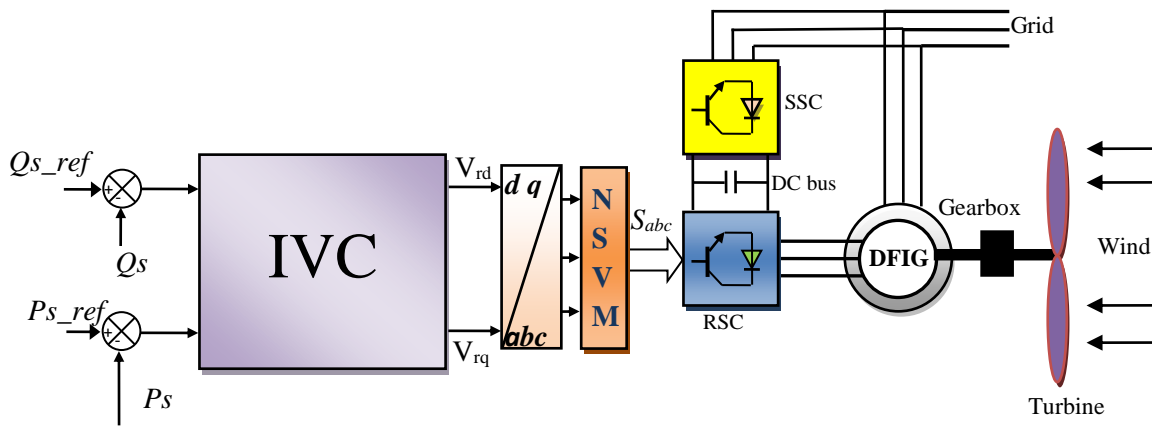


Fig. 8. Block diagram of DVC control with NSVM inverter.

5. SIMULATION RESULTS

In this part, simulations are carried out with a 1.5MW DFIG machine attached to a 398V/50Hz grid, using the Matlab/Simulink. Parameters of the DFIG are given in Table. 2. Two command schemes, DVC-3L-NSVM and DVC-PWM, are simulated and compared regarding reference tracking, powers ripples, stator current harmonics distortion, and robustness against DFIG parameter variations.

5.1. Reference Tracking Test (RTT)

Figs. 9-10 illustrate the harmonic spectrums of one phase rotor current of the 1.5MW DFIG for IVC-5L-SVM and IVC-5L-NSVM one respectively. Table 3 shows the comparative analysis of THD value. It can be deduced that the THD is minimized for IVC-5L-NSVM command (THD = 0.12%) when compared to IVC-5L-SVM (THD = 0.74%).

Figs. 11-16 show the obtained simulation results. For the proposed command strategies, the stator active

and stator reactive power tracks almost perfectly their references values. Moreover, the IVC-5L-NSVM command minimized the powers ripples and torque ripple compared to the IVC-5L-SVM command scheme (See Figs. 13-16).

Table 2. The DFIG Parameters.

| Parameters | Rated Value | Unity |
|----------------|-------------|-------------------|
| P | 1.5 | MW |
| V _s | 398 | V |
| F _s | 50 | Hz |
| P | 2 | |
| R _s | 0.012 | Ω |
| R _r | 0.021 | Ω |
| L _s | 0.0137 | H |
| L _r | 0.0136 | H |
| M | 0.0135 | H |
| J | 1000 | Kg m ² |
| f | 0.0024 | Nm/s |

Table 3. Comparative analysis of THD value (RTT)

| | THD (%) | |
|----------------------|------------|-------------|
| | IVC-5L-SVM | IVC-5L-NSVM |
| rotor current | 0.74 | 0.12 |

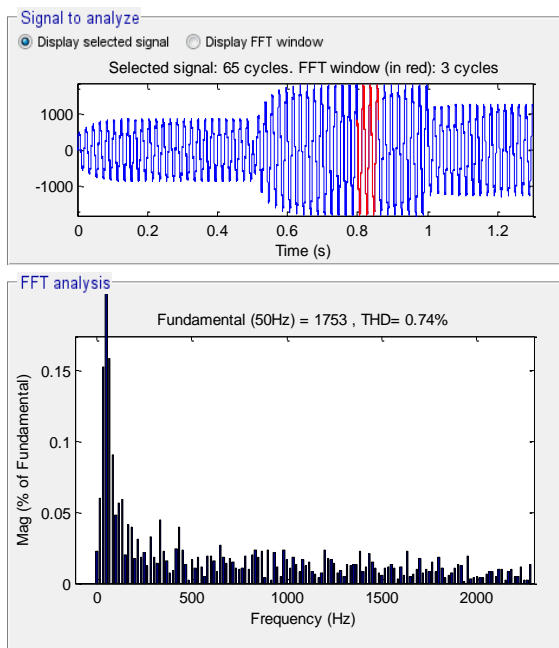


Fig. 9. THD of one phase rotor current for IVC-5L-SVM control (RTT).

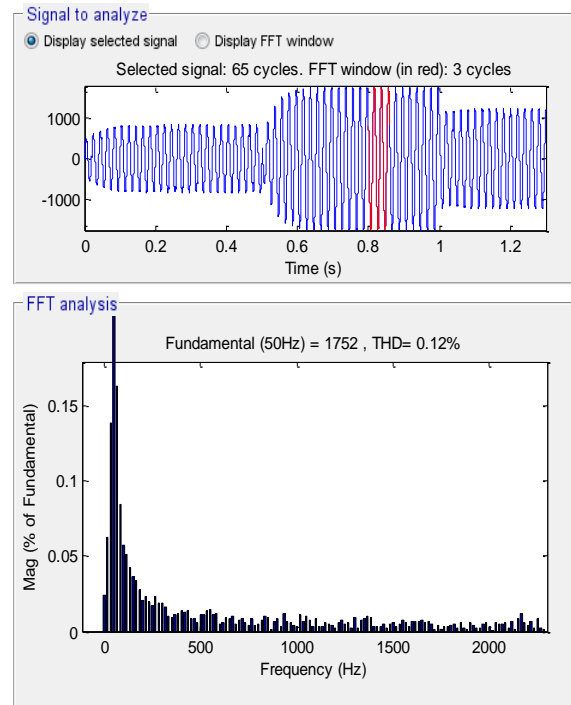


Fig. 10. THD of one phase rotor current for IVC-5L-NSVM control (RTT).

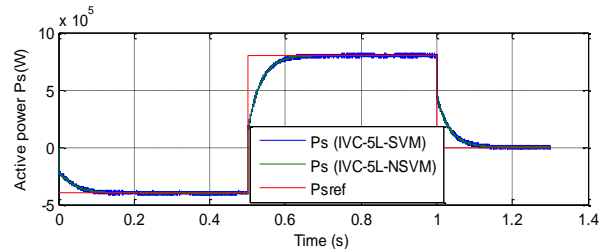


Fig. 11. Active power (RTT).

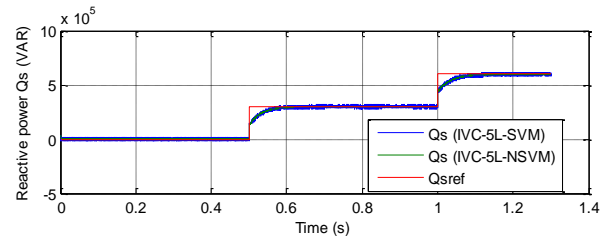


Fig. 12. Reactive power (RTT).

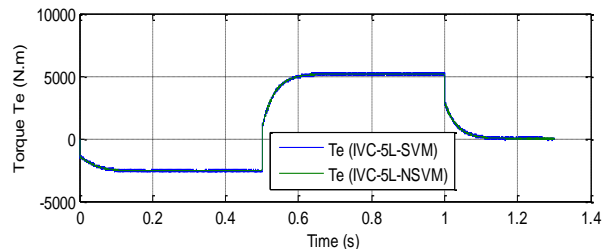


Fig. 13. Torque (RTT).

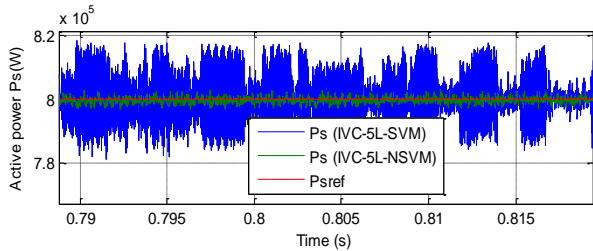


Fig. 14. Zoom in the active power (RTT).

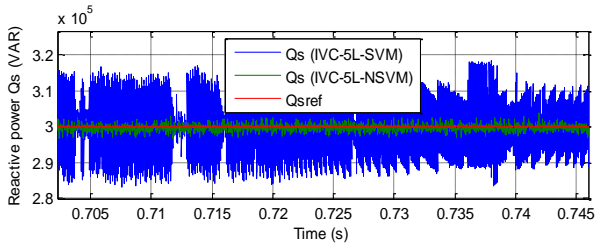


Fig. 15. Zoom in the reactive power (RTT).

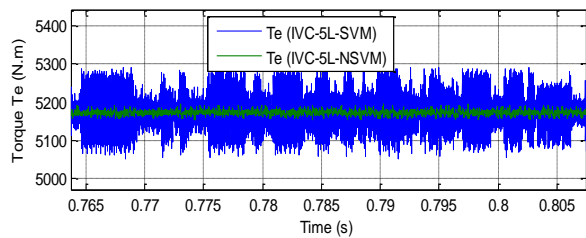


Fig. 16. Zoom in the torque (RTT).

5.2. Robustness Test (RT)

In this part, the nominal value of the R_r and R_s is multiplied by 2, the values of inductances L_s , M , and L_r are multiplied by 0.5. Simulation results are presented in Figs. 17-24. As it's shown by these figures, these variations present a clear effect on the stator active power, stator reactive power, and electromagnetic torque curves and that the effect appears more important for the IVC-5L-SVM command compared to IVC-5L-NSVM command (see Figs. 22-24). On the other hand, the THD value of rotor current in the IVC-5L-NSVM has been minimize significantly. Table 4 shows the comparative analysis of THD value. Thus it can be concluded that the IVC-5L-NSVM command is more robust than the IVC-5L-SVM command.

Table 4. Comparative analysis of THD value (RT),

| | THD (%) | |
|----------------------|------------|-------------|
| | IVC-5L-SVM | IVC-5L-NSVM |
| Rotor current | 1.81 | 0.36 |

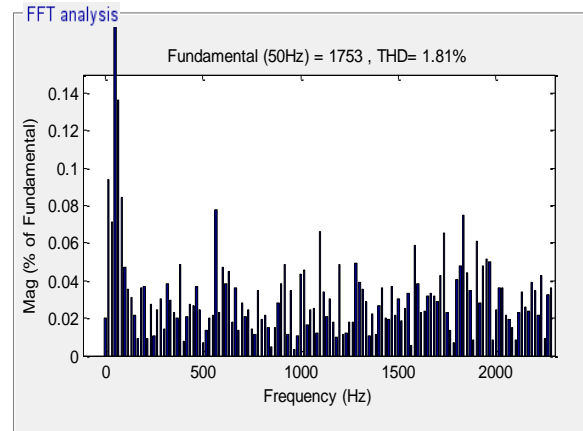
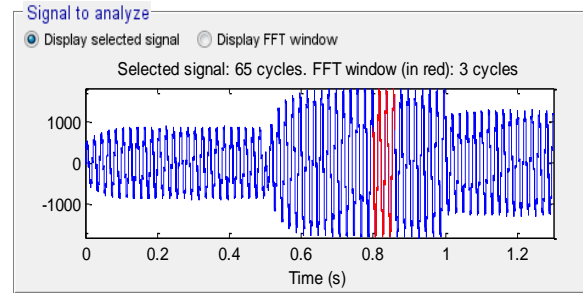


Fig. 17. THD of one phase rotor current for IVC-5L-SVM control (RT).

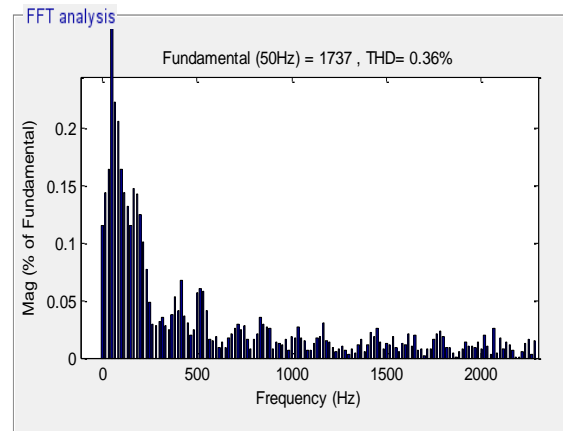
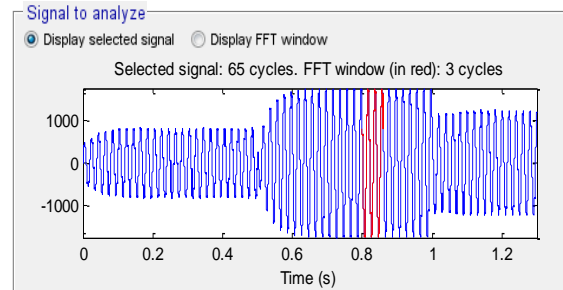


Fig. 18. THD of one phase rotor current for IVC-5L-NSVM control (RT).

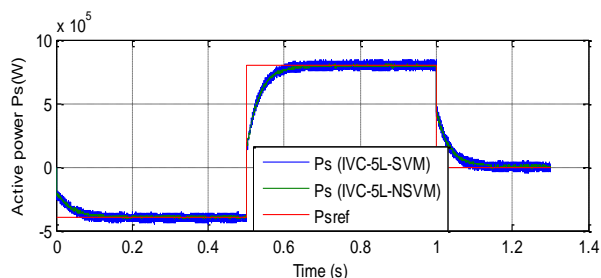


Fig. 19. Active power (RT).

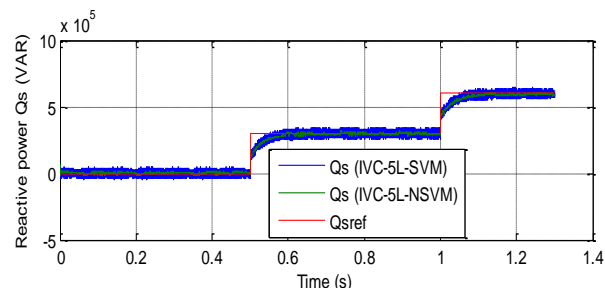


Fig. 20. Reactive power (RT).

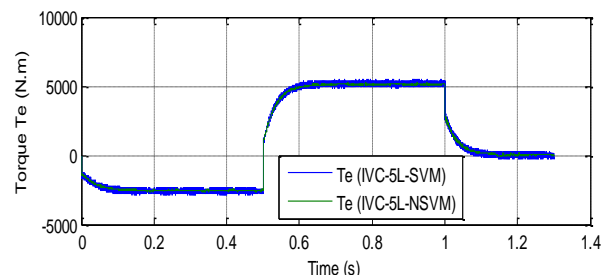


Fig. 21. Torque (RT).

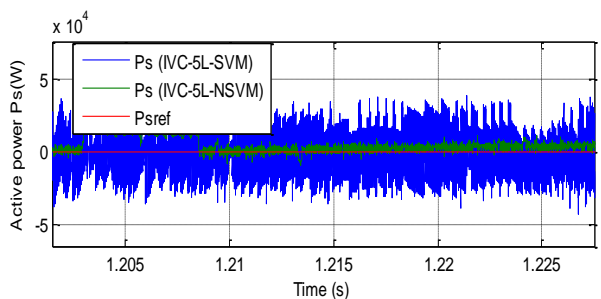


Fig. 22. Zoom in the active power (RT).

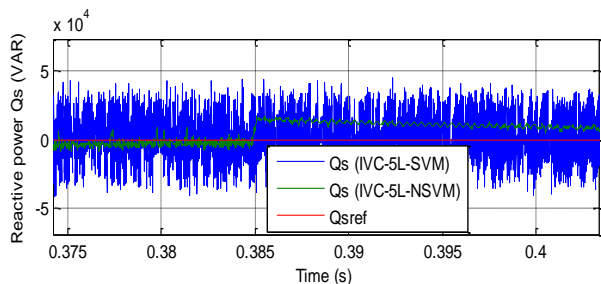


Fig. 23. Zoom in the reactive power (RT).

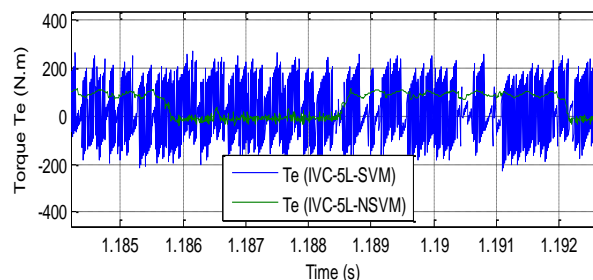


Fig. 24. Zoom in the torque (RT).

6. CONCLUSION

This work presents a IVC command of a DFIG using five-level SVM based on artificial neural networks controllers compared to five-level SVM inverter. With results obtained from the simulation, it was clear that for the similar operation conditions, the IVC command with five-level NSVM presents high-quality performance compared to the IVC using a five-level SVM and that was clear in the THD of rotor current in which the use of the 5L-NSVM has minimized the THD more than the 5L-SVM inverter.

REFERENCES

- [1] F. Amrane, A. Chaiba, "A Novel Direct Power Control for Grid-Connected Doubly Fed Induction Generator Based on Hybrid Artificial Intelligent Control with Space Vector Modulation", *Rev. Roum. Sci. Techn.-Electrotechn. Et Energ.*, Vol. 61, No. 3, pp. 263-268, 2016.
- [2] J. Mohammadi, S. Vaez-Zadeh, S. Afsharnia, E. Daryabeigi, "A Combined Vector and Direct Power Control for DFIG-based wind Turbines", *IEEE Transactions on Sustainable Energy*, Vol. 5, No. 3, 2014.
- [3] X. Zhu, S. Liu, Y. Wang, "Second-order Sliding-Mode Control of DFIG-based Wind Turbines", *IEEE 2014 3rd Renewable Power Generation Conference*, pp. 1-6, 24-25 September 2014.
- [4] D. Kanimozhi, S. Saravanan, R. Satheeshkumar, "Analysis of Doubly Fed Induction Generator Connected Matrix Converter in Wind Farm", *International Journal of Engineering Research & Technology*, Vol. 2, pp. 3981-3988, 2013.
- [5] F. Bishwang, T. Guanzheng, F. Shaosheng, "Comparison of Three Different 2-D Space Vector PWM Algorithms and their FPGA Implementations", *Journal of Power Technologies*, Vol. 94, No. 3, pp. 176-189, 2014.
- [6] M. Gaballah, M. El-Bardini, S. Sharaf, M. Mabrouk, "Implementation of Space Vector-PWM for Driving Two Level Voltage Source Inverters", *Journal of Engineering Sciences*, Vol. 39, No. 4, pp. 871-884, 2011.
- [7] H. Obdan, M. C. Ozkiloglu, "Performance Comparison of 2-level and 3-level Converters in a Wind Energy Conversion System", *Rev. Roum. Sci. Techn.-Electrotechn. Et Energ.*, Vol. 61, No. 4, pp. 388-393, 2016.

- [8] E. E. M. Mohamed, M. A. Sayed, “**Matrix Converters and Three-Phase Inverters Fed Linear Induction Motor Drives-Performance Compare**”, *Ain Shams Engineering Journal*, Vol. 2, pp. 1-12, 2016.
- [9] H. Benbouhenni, Z. Boudjema, A. Belaidi, “**Direct Vector Control of a DFIG Supplied By An Intelligent SVM Inverter For Wind Turbine System**”, *Iranian Journal of Electrical and Electronic Engineering*, In Press, 2018.
- [10] H. Benbouhenni, Z. Boudjema, A. Belaidi, “**Neuro-Second Order Sliding Mode Control of a DFIG Supplied by a two-level NSVM Inverter For Wind Turbine System**”, *Iranian Journal of Electrical and Electronic Engineering*, In Press, 2018.
- [11] M. Hasni, Z. Mancer, S. Mekhtoub, S. Bacha, “**Parametric Identification of the Doubly Fed Induction Machine**”, *Energy Procedia*, Vol. 18, pp. 177-186, 2012.
- [12] E. Bounadja, A. Djahbar, Z. Boudjema, “**Variable Structure Control of a Doubly Fed Induction Generator for Wind Energy Conversion Systems**”, *Energy Procedia*, Vol. 50, pp. 999-1007, 2014.
- [13] Z. Boudjema, A. Meroufel, E. Bounadja, Y. Djerriri, “**Nonlinear Control of a Doubly Fed Induction Generator Supplied by a Matrix Converter for Wind Energy Conversion Systems**”, *Journal of Electrical Engineering*, Vol. 14, No. 2, 2014.
- [14] K. Kerrouche, A. Mezouar, Kh. Belkacem, “**Decoupled Control Of Doubly Fed Induction Generator by Vector Control for Wind Energy Conversion System**”, *Energy Procedia*, Vol. 42, pp. 239-248, 2013.
- [15] A. Medjber, A. Moualdia, A. Mellit, M. A. Guessoum, “**Comparative Study Between Direct And Indirect Vector Control Applied to A Wind Turbine Equipped with A Double-Fed Asynchronous Machine Article**”, *International Journal of Renewable Energy Research*, Vol. 3, No. 1, pp. 88-93, 2013.
- [16] B. Karima, A. Boukhelifa, “**Output Power Control of A Variable Wind Energy Conversion System**”, *Rev. Roum. Sci. Techn.-Electrotechn. Et Energ*, Vol. 62, No. 2, pp. 197-202, 2017.